SMJ Saratov Medical Journal
ISSN 2712-8253, Saratov Medical Journal
2026. Volume 7. Issue 1. Article CID e0103
DOI: 10.15275/sarmj.2026.0103

Original article

Estimating coupling strengths between the branches of sympathetic control in a mathematical model of circulation using deep learning approach

Anna M. Vakhlaeva [1], Yury M. Ishbulatov [1, 2], ✉, Elizaveta S. Dubinkina [1], Boris P. Bezruchko [1, 2], Anatoly S. Karavaev [1, 2]
✉ ishbulatov95@mail.ru

[1]Chernyshevsky National Research University, Saratov, Russia
[2]Saratov Branch of the Institute of Radio Engineering and Electronics, Russian Academy of Sciences, Saratov, Russia

Received 12 January 2026, Accepted 6 March 2026

Abstract:
Directional coupling diagnostics is a promising method for the early noninvasive diagnosis of cardiovascular diseases. However, the complexity of living systems imposes unique requirements, necessitating the development of specialized approaches. This study explored the feasibility of solving the problem of directional coupling diagnostics using deep machine learning methods. Three fundamentally different artificial neural network architectures were considered: fully connected, recurrent, and convolutional. These architectures were compared for the accuracy of estimating the strength of directional coupling and their robustness to noise typically present in actual cardiac signals. The artificial neural networks were trained and tested on synthetic data: time series generated by functional mathematical models simulating the low-frequency oscillatory components of actual heart rate variability and mean blood pressure (Mayer waves). The fully connected artificial neural networks achieved an error of less than 3% when analyzing signals lasting only 70 seconds. The obtained results are promising in terms of the development of noninvasive methods for monitoring the state of autonomic circulatory control and for the advance of personalized medicine.

Keywords: directional coupling; mathematical modeling; deep learning; cardiovascular system

Cite as: Vakhlaeva AM, Ishbulatov YuM, Dubinkina ES, Bezruchko BP, Karavaev AS. Estimating coupling strengths between the branches of sympathetic control in a mathematical model of circulation using deep learning approach. *Saratov Medical Journal* 2026; 7 (1): e0103. https://doi.org/10.15275/sarmj.2026.0103

Introduction

Several studies suggest that sympathetic regulation of heart rate and mean arterial pressure represent two separate autonomic control loops. These loops influence each other (i.e., they are coupled), and the strength of their coupling reflects the dynamics of autonomic circulatory control [1]. This hypothesis can explain a number of experimental phenomena, such as prolonged periods of asynchronous behavior of the aforementioned sympathetic branches [2], while coupling strength has been shown to be a useful indicator of cardiovascular health [3].

Sympathetic control is often modeled as a closed-loop control system, also known as feedback control. Nonlinear dynamics provides several algorithms for detecting and measuring coupling between closed-loop control systems, including the phase dynamics modeling approach [4,5], linear and nonlinear approaches [6] based on Granger causality, nonlinear correlation [7], etc. However, the cardiovascular system is highly complex, and cardiovascular signals are often short, noisy, and broadband, making general approaches unreliable. Hence, detecting couplings between branches of the sympathetic regulation of blood circulation requires a specialized approach.

We previously confirmed that deep learning algorithms can be trained to solve a simpler classification task such as detecting the presence of a coupling [8] between two signals. In this study, we consider a more complex regression problem: estimating the precise strengths of the coupling between two signals. We also examine the robustness of the deep learning approach to colored noise, which is typical in real-world biological data. The algorithm was trained and tested on a pair of unidirectionally coupled oscillators modeling (LF) fluctuations in heart rate variability and mean arterial pressure, i.e., Mayer waves.

Materials and Methods

Mathematical model. Training and validation signals

Each deep learning algorithm requires a significant amount of training data, which is often difficult or even impossible to obtain due to patient risk, disease rarity, cost, or logistical issues. Here, we address this problem by training an algorithm for estimating coupling strengths on synthetic data generated using a mathematical model. The object of modeling is the dynamics of sympathetic regulation of heart rate and mean arterial pressure. In biophysical terms, both systems are often modeled as a pair of closed-loop control systems (oscillators) that generate periodic oscillations with a frequency of approximately 0.1 Hz. Fluctuations can also be observed in real-world heart rate variability and mean arterial pressure data (Mayer waves). Several studies have

also shown [1–3] that oscillators are coupled. To model coupled sympathetic regulation loops, we used van der Poll oscillators, which are a common simple model for oscillatory biological signals [9].

$$\begin{cases} \ddot{MAP}(t) - \mu(1 - MAP(t))\dot{MAP}^2(t) + (1 - 0.5\Delta)MAP(t) = 0 \\ \ddot{HRV}(t) - \mu(1 - HRV(t))\dot{HRV}(t)^2 + (1 - 0.5\Delta)HRV(t) + \varepsilon\left(HRV(t) - MAP(t)\right) = 0 \end{cases} \quad (1)$$

Where MAP(t) is the LF component of mean arterial pressure, HRV(t) is the LF component of heart rate variability, μ = 2 is the nonlinearity parameter, Δ ∈ [-1:1.5] is the frequency detuning between the oscillators, and ε ∈ [0.005:0.5] is the coupling coefficient. System (1) was integrated using the Euler method with an integration step of 0.004, and the data were subsequently resampled at a frequency of 10 samples per second. Examples of the MAP(t) and HRV(t) signals are shown in *Figure 1*. Clearly, the signals reproduce the main spectral characteristics of the corresponding real-world signals in the LF range: pronounced oscillations with a frequency of approximately 0.1 Hz.

We generated 18,000 pairs of MAP(t) and HRV(t) signals:

9,000 pairs with ε=0 (i.e. no coupling), 7,000 pairs were included in the training dataset, and the remainder in the validation dataset;

9,000 pairs with ε ∈ [0.005:0.5] and Δ ∈ [-1:1.5], 7,000 pairs were included in the training dataset, and the remainder in the validation dataset;

There were no repeating (ε, Δ) pairs, while (ε, Δ) pairs that resulted in synchronization between oscillators were excluded, as this is another issue that we decided to investigate in future studies. To detect synchronization, we used the Hilbert transform to introduce the phases of both oscillators and then calculated the phase difference. In the case of phase synchronization, the phase difference is constant, i.e., it is parallel to the x-axis (time). In the absence of synchronization, the phase difference is tilted. To estimate the phase difference angle, we approximated it with a straight line and measured the angle coefficient. An angle coefficient less than 0.05 (the value was estimated empirically) served as our synchronization marker.

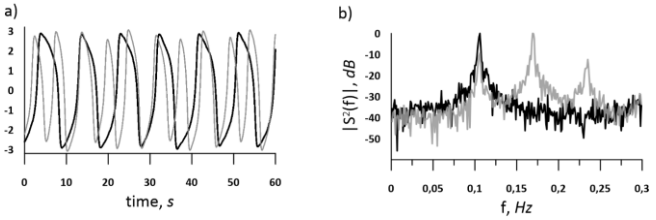

Figure 1. Time series and power spectra for modeled HRV and MAP signals

Testing signals

Artificial deep neural networks, trained and validated on data generated by system (1), were tested on a signal generated separately using system (2):

$$\begin{cases} \ddot{MAP}(t) - \mu\left(1 - MAP(t)\right)^2\dot{MAP}(t) + (1 - 0.5\Delta)MAP(t) + \xi_1(t) = 0 \\ \ddot{HRV}(t) - \mu\left(1 - HRV(t)\right)^2\dot{HRV}(t) + (1 - 0.5\Delta)HRV(t) + \varepsilon\left(HRV(t) - MAP(t)\right) + \xi_2(t) = 0 \end{cases} \quad (2)$$

Where ξ_1 (t) and ξ_2 (t) are independent realizations of colored (red) zero-mean Gaussian noise generated as follows:

$$\xi_{(n+1)} = 0.97\xi_n + \zeta_n, \quad (3)$$

Where ζ is white zero-mean Gaussian noise. The spectral properties of noise (3) correspond to stochastic components extracted from real-world heart rate variability and blood pressure signals.

We generated 1,000 pairs of MAP(t) and HRV(t) signals by coupled oscillators (2) and 1,000 pairs of signals using uncoupled oscillators, for each noise level (25%, 50%, and 100%). Noise level was measured as the ratio of the standard deviations of the noise per se to the signal before noise.

Artificial neural networks

Three types of artificial neural networks (ANNs) were considered: fully connected (FNN), convolutional (CNN), and recurrent (RNN). For each type, several architectures of varying complexity (number of hidden layers and neurons per layer) were explored. The results showed that after a certain complexity threshold was reached, further increases did not improve performance. Therefore, only minimally sufficient models (one for each type) were discussed. The input layer (a 700×2 matrix) was identical for all networks. The top row contained 70 seconds of MAP(t) signals (~5–12 periods), while the bottom row contained 70 seconds of HRV(t) signals. As previously shown [7], longer time series do not improve performance but rather unnecessarily complicate the networks. The ReLU activation function was employed in the input and hidden layers. For the FNN model, we chose a structure with six hidden layers:

Input layer with 700×2 input data shape;

Input smoothing layer;

Six fully connected layers with 600, 400, 300, 200, 100, and 50 neurons;

Output fully connected layer with one neuron and a linear activation function.

For the CNN model, we used the following structure:

Input layer with 700×2 input data shape;

2D convolutional layer with 32 filters and a 2×50 kernel, max pulling layer with a 2×2 kernel;

2D convolutional layer with 128 filters and a 2×25 kernel, max pulling layer with a 2×25 kernel;

2D convolutional layer with 158 filters and a 2×12 kernel, max pulling layer with a 2×12 kernel;

2D convolutional layer with 124 filters and a 2x6 kernel, max pulling layer with a 2x6 kernel;

Input smoothing layer;

A fully connected layer with 32 neurons;

Output fully connected layer with one neuron and a linear activation function.

In the RNN model, we used the following structure:

Input layer with 700x2 input data shape;

Five simple recurrent layers with 100, 120, 90, 70, and 60 neurons;

A fully connected layer with 40 neurons;

A fully connected layer with 20 neurons;

Output fully connected layer with one neuron and a linear activation function.

In supervised learning, the mean absolute error (MAE) of the coupling coefficient ε estimates was minimized using the RMSprop optimization algorithm. Training was conducted for 30 epochs without early stopping or additional regularization. After each epoch, the neural networks were tested on the validation dataset, and the validation results and corresponding weights were saved in a temporary file. Ultimately, we selected the weights that demonstrated the best results on the validation dataset.

Results

The results are presented in *Figures 2, 3,* and *Table*. *Figure 2* illustrates the performance of the neural networks on the entire test dataset, i.e., ε ∈ [0.005:0.5] and Δ ∈ [-1:1.5]. *Figure 3* shows the performance of the neural networks on a smaller subset of the training dataset, where ε ∈ [0.005:0.1] and Δ ∈ [-1:1.5].

RNN demonstrates the worst robustness to noise among all neural networks; the estimated and true ε values show no obvious correlation even with the weakest 25% noise (*Table*). Both FNN and CNN demonstrate similar variance in estimates, but FNN has a lower average median error, especially at 100% noise. For FNN, the Q1 and Q3 values of the median error distribution also do not exceed 3%. All ANNs (especially CNN) tend to overestimate stronger coupling.

Figure 4 compares FNN with other classical approaches to estimating coupling strength, viz., cross-correlation and phase dynamics modeling (γ-index). Neither approach can provide direct estimates of ε, only indices proportional to ε. Therefore, Figure 4 shows the relationships between the true ε and the index values returned by these methods. *Figure 4* shows that the phase dynamics modeling approach and cross-correlation return indices that are generally proportional to ε. However, these relationships are nonlinear, and both methods cannot withstand 100% noise. In the case of FNN, the ε estimates exhibit a strong linear correlation with the true value, but the FNN overestimates the stronger ε, which is consistent with the results presented in *Figure 2*.

Discussion

Our study has several limitations. We have not yet considered cases involving chaotic oscillators or bidirectional coupling. Studying other types of ANNs, such as reservoir computing, would also benefit our research. Performance may be further improved by introducing noise into the training dataset. All these issues require further investigation; however, the current results are quite promising.

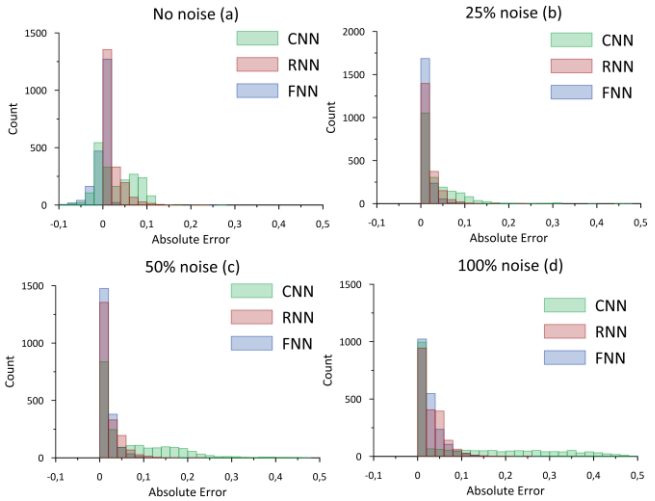

Figure 2. Histograms of absolute errors in estimating the coupling strength ε using CNN (green), RNN (red), and FNN (blue) with no noise in the system dynamics (panel a), with 25% noise (panel b), with 50% noise (panel c), and with 100% noise (panel d)

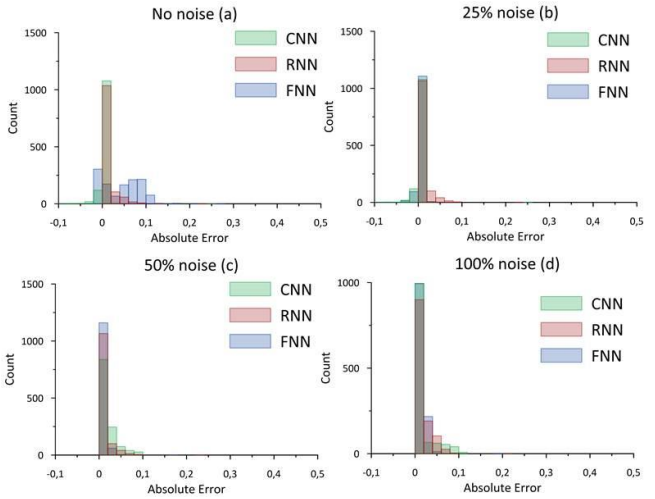

Figure 3. Histograms of absolute errors in estimating the strength of weak coupling (ε < 0.1) using CNN (green), RNN (red), and FNN (blue) with no noise in the system dynamics (panel a), with 25% noise (panel b), with 50% noise (panel c), and with 100% noise (panel d)

Table. Median error of ε estimates for each tested artificial neural network, including fully connected (FNN), convolutional (CNN), and recurrent neural network (RNN), for different noise levels (0-100%)

Noise, %	FNN, %	CNN, %	RNN, %
0	0.15 (-1.88, 0.15)	-0.07 (-0.07, 0.00)	0.05 (-7.91, 0.05)
25	0.17 (0.17, 2.34)	0.20 (0.20, 5.60)	0.00 (-19.87, 21. 04)
50	0.17 (0.17, 2.01)	0.20 (0.20, 5.82)	0.00 (-20.00, 19.62)
100	0.17(-3, 2.7)	0.67 (0.20, 8.01)	-0.01 (-18.02, 24.70)

The median error is shown as the average median error (Q1, Q2), normalized to 0.5 and expressed as a percentage

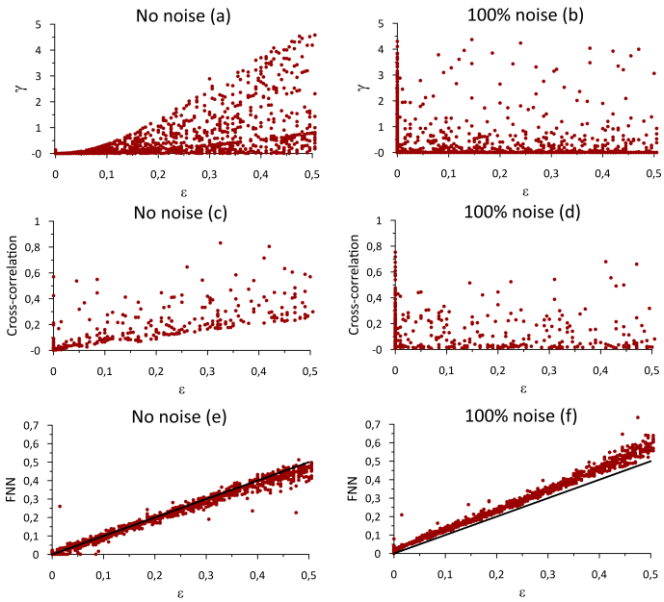

Figure 4. Absolute values of the indices obtained using phase dynamics modeling (γ), the maximum cross-correlation function, and a fully connected neural network (FNN) when estimating coupling strength. The values are plotted against the true value ε. Panels on the left show estimates performed without noise in the system dynamics, while panels on the right show estimates in the presence of 100% noise in the system dynamics. Panels (a, b) show phase dynamics simulations, panels (c, d) show cross-correlation, and panels (e, f) show a fully connected neural network. The black lines in panels (e, f) show diagonal lines.

Van der Pol oscillators are still very simple models, even though they reproduce the general shape of the LF oscillations generated by coupled sympathetic regulation loops of heart rate and mean arterial pressure. They do not reproduce the shape of unfiltered ECG and arterial pressure signals, the spectra are not broadband, and they lack VLF and HF components. Therefore, the next step in our research is to develop models that quantitatively reproduce the shape, spectral, and phase properties of actual cardiovascular signals, particularly blood pressure and ECG signals. We hope that a coupling detection algorithm based on deep learning can be trained on such model data and then employed for real-world signals. There are successful examples of applying transfer learning to cardiovascular data, e.g., in the diagnosis of coronary artery disease, heart rate detection, and signal segmentation [10]. However, to date, no attempts have been made to estimate more complex nonlinear metrics, such as directional coupling.

These results can be used to develop personalized and preventive medicine, and to extract diagnostic information from noninvasive signals that can be monitored using wearable devices such as smartwatches and fitness trackers.

Conclusion

We trained ANNs to estimate the strength of the directional coupling between two branches of the sympathetic regulation of blood circulation in a simple mathematical model. The networks were trained on short simulated signals representing LF fluctuations in mean blood pressure and heart rate variability, which are typically associated with the dynamics of sympathetic regulation.

We compared the performance of FNNs, CNNs, and RNNs, including their robustness to noise. We also compared the performance of ANNs with a well-established approach to estimating coupling strength via modeling phase dynamics and cross-correlation:

- FNNs and CNNs demonstrated good robustness to noise, especially when estimating the strength of weaker connections;
- FNNs exhibited the best overall performance, with the median error not exceeding 3% of the maximum ε value;
- All results were obtained on relatively short signals (70 seconds).

Despite the limited scope of this study, we believe the results are promising for the development of noninvasive cardiovascular health monitoring and personalized medicine.

Acknowledgments

This study was supported by the Russian Science Foundation, project No. 25-72-00158, https://rscf.ru/project/25-72-00158/.

Conflict of interest

The authors declare that they have no conflicts of interest.

Ethics statement

This article is not based on any studies with human participants conducted by any of the authors and therefore does not require ethical approval.

References

1. Karavaev AS, Skazkina VV, Borovkova EI,, et al. Synchronization of the processes of autonomic control of blood circulation in humans is different in the awake state and in sleep stages. *Frontiers in Neuroscience* 2022; 15: 791510. https://www.doi.org/10.3389/fnins.2021.791510.
2. Kiselev AR, Borovkova EI, Simonyan MA, et al. Autonomic control of cardiorespiratory coupling in healthy subjects under moderate physical exercises. *Russian Open Medical Journal* 2019; 8(4): 0403. https://www.doi.org/10.15275/rusomj.2019.0403
3. Kiselev AR, Gridnev VI, Prokhorov MD, et al. Evaluation of 5-year risk of cardiovascular events in patients after acute myocardial infarction using synchronization of 0.1-Hz rhythms in cardiovascular system. *Annals of Noninvasive Electrocardiology* 2012 17(3): 204-213. https://www.doi.org/10.1111/j.1542-474X.2012.00514.x
4. Smirnov DA. Generative formalism of causality quantifiers for processes. *Physical Review E*. 2022; 105: 034209. https://www.doi.org/10.1103/PhysRevE.105.034209
5. Borovkova EI, Dubinkina ES, Hramkov AN, et al. Study of statistical properties of the method of analysis of directional couplings based on modeling of phase dynamics. *Proceedings of SPIE* 2022; 12194: 121940B. https://www.doi.org/10.1117/12.2626038.
6. Wismüller A, Dsouza AM, Vosoughi MA, Abidin A. Large-scale nonlinear Granger causality for inferring directed dependence

from short multivariate time-series data. *Scientific Reports* 2021; 11: 7817. https://www.doi.org/10.1038/s41598-021-87316-6
7. Wang T, Shiqiang Z. Study on linear correlation coefficient and nonlinear correlation coefficient in mathematical statistics. *Studies in Mathematical Sciences* 2011; 3(1): 58-63. https://www.doi.org/10.3968/j.sms.1923845220110301.4Z483
8. Vakhlaeva AM, Ishbulatov YuM, Dubinkina ES, et al. Application of neural networks to detection of unidirectional coupling between Van der Pol oscillators from ultrashort time series in the presence of noise. *The European Physical Journal Special Topics* 2025; 234: 4001–4007. https://www.doi.org/10.1140/epjs/s11734-025-01592-1.
9. Kaplan BZ, Gabay I, Sarafian G, Sarafian D. Biological applications of the "Filtered" Van der Pol oscillator. *Journal of the Franklin Institute* 2008; 345(3): 226-232. https://www.doi.org/10.1016/j.jfranklin.2007.08.005.
10. Mazumder O, Banerjee R, Roy D, et al. Synthetic PPG signal generation to improve coronary artery disease classification: Study with physical model of cardiovascular system. *Journal of Biomedical and Health Informatics* 2022; 26 (5): 2136-2146. https://www.doi.org/10.1109/JBHI.2022.3147383.

Authors:
Anna M. Vakhlaeva – MSc Student, Department of Dynamical Modeling and Biomedical Engineering, https://orcid.org/0009-0009-3079-188X;
Yury M. Ishbulatov – PhD, Associate Professor, Department of Dynamical Modeling and Biomedical Engineering, https://orcid.org/0000-0003-2871-5465;
Elizaveta S. Dubinkina – Undergraduate Student, Department of Dynamical Modeling and Biomedical Engineering, https://orcid.org/0000-0002-4636-3937;
Boris P. Bezruchko – DSc, Professor, Department of Dynamical Modeling and Biomedical Engineering, https://orcid.org/0000-0002-6691-8653;
Anatoly S. Karavaev – DSc, Chair of the Department of Dynamical Modeling and Biomedical Engineering, https://orcid.org/0000-0003-4678-3648.